

Detonation Failure Characterization of Homemade Explosives

Robert S. Janesheski,^[a] Lori J. Groven,^[a] and Steven F. Son^{*[a]}

Abstract: Typically, characterizing home made explosives (HMEs) requires many large scale experiments, which is prohibitive given the large number of materials in use. A small scale experiment was developed to characterize HMEs such as ammonium nitrate-fuel oil mixtures. A microwave interferometer is applied to small scale confined transient experiments, yielding time resolved characterization of a failing detonation that is initiated with an ideal explosive booster charge. Experiments were performed with ammonium nitrate and two fuel compositions (diesel fuel and mineral oil). It was observed that the failure dynamics were influenced by factors such as the chemical composition, confiner thickness, and applied shock wave strength. Thin steel walled confiners with 0.71 mm wall thickness experienced

detonation failure and decoupling of the shock wave from the reaction zone. Confiners with a wall thickness of 34.9 mm showed a decrease in propagation speed and a steady reactive wave was achieved. Varying the applied shock strength by using an attenuator showed corresponding changes in the initial overdriven reactive wave velocity in the HMEs. The distance to detonation failure was also shown to depend on the attenuator length when thin wall confinement was used. This experimental method is shown to be repeatable and can be performed with little required material (about 2 g). The data obtained could be useful to model development and validation, as well as quantifying detonability of materials.

Keywords: Home made explosives • Ammonium nitrate • Microwave interferometry • Detonation failure • Shockwave

1 Introduction

There is a strong need for characterizing, modeling, and understanding home made explosives (HMEs) as their availability and low cost makes them terrorist accessible [1–5]. In order to more adequately mitigate and respond to these threats, characterization coupled with modeling of HMEs has become of the utmost importance. Presently, the lack of detailed experimental data has limited the development of reactive models for HMEs. This is especially challenging because of the wide variety in HME compositions and typically expensive, large scale experiments currently applied.

A large critical diameter is a characteristic associated with many HMEs due to a thick reaction zone. An explosive with a large critical diameter is also termed a non-ideal high explosive. Ammonium nitrate (AN), a typical HME component, has a critical diameter of 100 mm when confined in a steel tube that is loosely packed [6]. When fuel is added to AN, it has been shown that the critical diameter can vary from 10 mm (fine AN) up to 50 mm (course AN) [7]. Many parameters such as AN particle size, confiner diameter, packing, and confiner thickness have an effect on the detonability of HMEs [2–4]. However, the wide range of HME compositions makes large scale characterization of every composition prohibitive.


A steady detonation experiment is the conventional approach for detonation property measurement such as velocity, reaction zone length, and detonation front curvature

[5]. Producing a steady detonation with a HME requires a large amount of material, on the order of kilograms, in order to satisfy the critical diameter constraint. It is evident that small scale experiments are highly desirable and the ability to assess detonability with small samples is also a critical need.

Transient data also provides rich data sets for model validation. The large scale required to sustain a detonation in HMEs has made it a challenge to perform transient measurements, such as deflagration to detonation transition (DDT) [8] or shock initiation [9]. Shock initiation measurements have been used for the calibration of parameters for reaction models [9], such as Forest-Fire [10] and ignition and growth [11], typically used for ideal explosives.

The data available involving transient measurement during a reactive wave transition (including detonation failure) for HMEs is very limited. However, some work has

[a] R. S. Janesheski, L. J. Groven, S. F. Son
School of Mechanical Engineering
Purdue University
500 N. Allison Rd.
West Lafayette IN 47907, USA
*e-mail: sson@purdue.edu

 Supporting information for this article is available on the WWW under <http://dx.doi.org/10.1002/prop.201300041> or from the author.

been performed to fit equation of state (EOS) parameters for HMEs using high pressure X-ray diffraction and gas gun-driven plate impact experiments [12]. Reaction and growth modeling parameters have also been measured with HMEs by using a hybrid Hopkinson bar experiment (modified plate impact experiment) [13]. The need for an experimental technique to study the transient dynamics of a HME remains, especially if the experiment can span a wide parameter space. A small scale transient experiment would be especially useful to modelers and could provide valuable qualitative insight as well.

Microwave interferometry has been used as a non-intrusive measurement for burning rates of propellants [14] and for the study of the detonation of ideal explosives including tetryl [15], trinitrotoluene (TNT), Pentolite, Amatol, and even Tritonal (an aluminized explosive) [16]. Low power microwaves have been used to develop interference signals produced from reflection off of the reactive wave front. The position and velocity of the reactive wave can then be calculated non-intrusively from the interference signal. The spatial and temporal resolution of the technique is dependent on the wavelength of the microwave system. Over the years, the technique has been refined and wavelengths have decreased from 3 cm [16] to 2 mm [17] resulting in increased accuracy. It also has been shown that a single experiment can measure the regression rate of propellants as a function of pressure [18] in a slowly pressurizing experiment. Since the technique is applicable to both deflagration and detonation, it has also been used to characterize the highly transient deflagration-to-detonation transition (DDT) of ideal explosives [8]. Therefore, this diagnostic tool could be applied to detonation failure in HMEs.

It is noted here for clarity that the term “detonation” is only applicable to a steady reactive wave involving a shock. Herein, we use the term “detonation failure” to refer to the transient reactive wave process where the reaction zone decouples from the leading shock wave. We use the term “reactive wave” to refer to the transient front observed.

The objective of this work is to develop a small scale experiment to characterize HMEs in a detonation failure experiment using a microwave interferometer. This could provide a broad range of parameter space for model validation or calibration, as well as provide a quick screening tool and increase the understanding of the reactive dynamics. Material composition, various confinement properties, and leading shock strength can also be investigated to quantify the effects on the failing detonation through HMEs.

2 Experimental Procedure

2.1 Materials and Equipment

The HMEs used in this work consisted of ammonium nitrate (AN) mixed with various fuels. Kinopak™ ammonium nitrate produced by SEC, Orica Manufacturing Company, was used. Sizing of the AN was conducted with a Malvern Mastersizer

with hexane as the dispersing medium. The material is trimodal with a mean volume diameter of ca. 200 μm and $d(50)$ of ca. 175 μm . Various weight percentages of diesel (Marathon Diesel) and mineral oil (PTI Process Chemicals, Ringwood, IL) were mixed with AN as the fuels of interest. In these experiments, 2–2.5 g of HME was required. The HME mixtures characterized in this work include AN with 2, 5, and 10 wt-% diesel fuel as well as AN with 2 and 15 wt-% mineral oil. The explosives were pressed within the confiner in increments to yield uniform density throughout the length of the sample. Depending on the compositions being pressed, 0.25 g increments were pressed to lengths that ranged from 5 to 10 mm. For all samples the density was typically 1.1 g cm^{-3} . This corresponds to ca. 60% TMD for compositions with 2 wt-% fuel to ca. 70% TMD for compositions with 15 wt-% fuel. Approximately 1.9 g of Primasheet 1000 (an ideal explosive with 63% PETN qualified to MIL-PRF-46676) was used to develop a steady detonation into the HME. A Teledyne Risi, Inc. RP-502 detonator was used to initiate the detonation in the Primasheet.

Three confinement conditions were used that included negligible confinement (polypropylene tube with a wall thickness of 0.2 mm and I.D. of 6.95 mm), thin-wall confinement (304 stainless steel tube with 0.71 mm wall thickness and I.D. of 6.53 mm) and thick-wall confinement (1018 steel tube with a wall thickness of 34.9 mm and I.D. of 6.35 mm). To study the effect of applied shock strength leading into the HMEs, poly(methyl methacrylate) (PMMA) attenuators with thicknesses ranging from 1 to 8 mm were used.

A custom built microwave interferometer was used to produce time-resolved position measurements of the reactive front, or shock wave. The microwave system produced microwaves with a frequency of 35 GHz and a free space vacuum wavelength of 8.6 mm. The output signal from the microwave interferometer was recorded with a 500 MHz sampling rate using a Tektronix DPO4034 Digital Oscilloscope. Microwave transmission to the sample was made possible by an expendable 6.35 mm O.D. cylindrical Teflon™ waveguide. The location of the reactive wave within the confiners was verified with a fiber optic system consisting of patch cables (Thorlabs, Inc. M34L02) having a 600 μm core diameter and DET10A photo-detectors (Thorlabs, Inc.) with a 1 ns rise time.

2.2 Experimental Configuration

The experimental configuration within the confiner is shown in Figure 1. Detonation begins with the detonator initiating a steady detonation through the ideal explosive. When present, a PMMA attenuator transmits a shock wave to the HME. The baseline configuration is to have no PMMA attenuator. When the attenuator was omitted, the ideal and HMEs were placed together to allow for the steady detonation developed by the ideal explosive to transition to the HME. Due to the inner diameter of the confin-

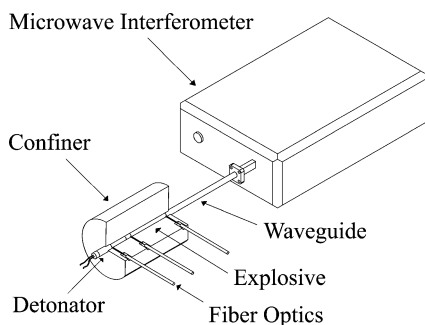


Figure 1. Schematic of the experimental configuration.

er being below the critical diameter for the HME, the initial overdriven reactive wave weakens and decelerates in the HME.

The waveguide was placed on the opposite end of the detonator in the confiner tube as shown in Figure 1. The explosives and PMMA attenuator are dielectric mediums, allowing for transmission of the microwave signal from the waveguide. Reflection of the microwave signal occurs with the presence of a dielectric discontinuity caused by an ionizing reaction zone or a shock wave [19,20]. A fiber optic cable was located at the interface of the detonator/ideal explosive to trigger the oscilloscope. A second fiber optic cable was placed at the ideal/HME interface. A third location was either at 1.5 cm away from the ideal/non-ideal interface into the HME for in situ interference signal calibration or at the end of the confiner to verify that a reactive wave was sustained through the entire length of the HME. Further details of the microwave interferometry technique applied to the collected data can be found in the Supporting Information.

2.3 Numerical Predictions

The Chapman-Jouguet (C-J) temperatures were predicted for a range of compositions using CHEETAH 6.0 with the standard equation of state product library [19]. Compositions for investigation were selected based on the predicted temperature; assuming that the failure dynamics of these HMEs would correlate to the predicted adiabatic temperatures. A density of 1.1 g cm^{-3} was assumed to match experiments. Predicted temperatures can be found in the Supporting Information (Figure S4).

Supporting Information (see footnote on the first page of this article): Further experiment details.

3 Results and Discussion

The results from a typical test, data verification, and data for experimental accuracy can be found in the Supporting Information and all analysis steps are detailed.

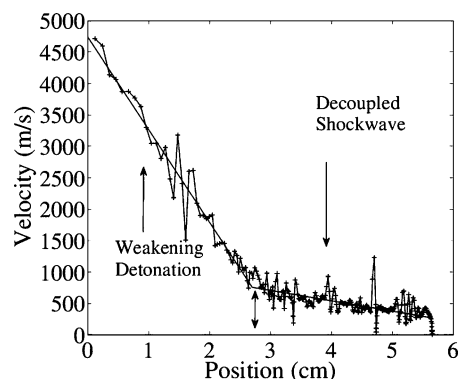


Figure 2. Wave velocity as a function of position through AN/2 wt-% diesel fuel.

3.1 Thin-Walled Confinement with AN/Diesel Compositions

A typical position vs. velocity result with AN/2 wt-% diesel fuel is shown in Figure 2. Two distinct slopes are observed. The initial slope is the weakening of the overdriven reactive wave as it travels through the AN/2 wt-% diesel fuel composition. The second velocity slope is less steep. The location of the interception of the two slopes is defined as the location, at which the reactive wave fails and measurement of a decoupled shock wave begins. The location is indicated in Figure 2. This is analogous to analysis of shock initiation to determine run-to-detonation, and here this could perhaps be termed a run-to-failure measure. It is not meant to be a precise measure of the point of failure, but rather is a systematic way to obtain a single parameter from an experiment. This value and the entire position-time trace are useful for model comparison.

The velocity oscillation may correspond to a pulsating, failing detonation (reactive wave). It is noted that once the shock wave decouples from the reaction, two microwave signals will be reflected and measured by the interferometer (one of reflection off of the reaction front and the other off of the shock wave). We do see some indications of this in the data, however the current method of processing the data did not allow for extracting the reaction front data from the mixed interference signal. Perhaps future work could analyze these results in order to separate the two signals and allow the relative velocities between the decaying reaction front and the shock wave to be determined. However, this is not a trivial task because after the shock the dielectric constant increases because the bed density is higher, effectively changing the wavelength.

The stoichiometric mixture of AN/diesel fuel was calculated to consist of 5.56 wt-% diesel fuel. Predictions using CHEETAH (see Supporting Information), indicated that the temperature is highest near the stoichiometric composition (near 5 wt-% diesel fuel). Ultimately failure is precipitated by a significant drop in reaction rate, which is a strong function of temperature. Therefore, higher predicted adia-

Table 1. Failure position and velocity measured at the location of the velocity slope intercepts for various AN/diesel fuel compositions.

Diesel fuel/[wt-%]	Position/[cm]	Velocity/[m s ⁻¹]
2	2.7	760
5	3.2	850
10	2.9	640

batic temperatures should lead to the reaction front being sustained further through the HME.

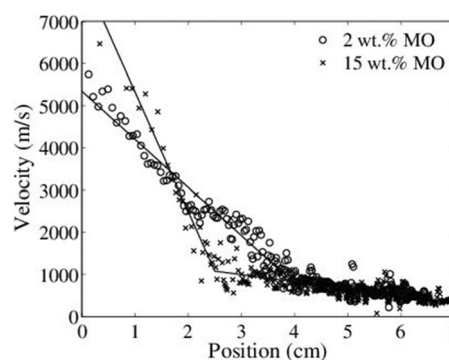
Measurements of the location within the HME where detonation fails and decoupling of the shock wave occurs (run-to-failure distance) are shown for compositions of AN with 2, 5, and 10 wt-% diesel fuel in Table 1 for thin wall confiners. It is shown that the mixture consisting of AN/5 wt-% diesel sustained a reactive wave the furthest into the HME. It is shown that the fuel lean (2 wt-% diesel) and fuel rich (10 wt-% diesel) were not able to sustain the reactive wave through the confiner. Consequently, we see that they run-to-failure. Measurements appear to be consistent with the idea that a higher temperature tends to lead to a longer run-to-failure distance.

For failed propagations, unreacted HME was recovered and was observed to be compacted due to the shock wave. The recovered samples after the experiments verified that the detonation failed in the HME. Obviously, deflagration also failed as would be expected for these materials in this configuration. All thin wall confinement experiments were consistent with complete failure. When the reactive wave fails the shock wave decouples and decreases in speed without the energy from the reaction zone, eventually weakening to the point where no deformation of the thin-wall confiner occurs. An example of a recovered thin walled steel confiner is shown in Figure 3.

The remaining lengths of the recovered confiners were measured and were approximately 3.9, 4.0, and 4.4 cm long for AN with 2, 5, and 10 wt-% diesel fuel, respectively. The recovered confiners show that deformation occurred further through the confiners for mixtures closest to stoichiometric. It is noted that these measurements are approximate and the microwave interferometer measurements are viewed as being more reliable.

3.2 Thin-Walled Confinement with AN/Mineral Oil Compositions

A similar relationship was seen when diesel fuel was replaced with mineral oil (MO). Velocity slope intercepts were used to determine the location of the reactive wave failure (run-to-failure) in the same way previously shown for AN/diesel fuel. Increasing the fuel percentage decreased how far the failing detonation could sustain itself through the HME, shown in Figure 4.

**Figure 3.** Recovered thin-walled confiner after detonation of a non-ideal explosive fails.**Figure 4.** Results showing the velocity of the detonation front through non-ideal explosives with various mineral oil compositions in thin-wall confiners (304 stainless steel tube with 0.71 mm wall thickness and I.D. of 6.53 mm).

The AN/2 wt-% MO composition sustained the reactive front through 3.9 cm of HME, while the AN/15 wt-% composition only sustained the reactive front for 2.5 cm, as shown in Table 2. Assuming that mineral oil is similar in composition to diesel fuel, it was shown that a mixture closer to the stoichiometric composition (2 wt-% MO) sustained the reactive wave further, much like what was previously observed for diesel fuel.

3.3 Various Confinement Conditions with AN/2 wt-% Mineral Oil

Different failure dynamics are observed when the material composition is held constant and the confinement condi-

Table 2. Failure position and velocity measured at the location of the velocity slope intercepts for various AN/mineral oil compositions.

Mineral oil/[wt-%]	Position/[cm]	Velocity/[m s ⁻¹]
2	3.9	910
15	2.5	980

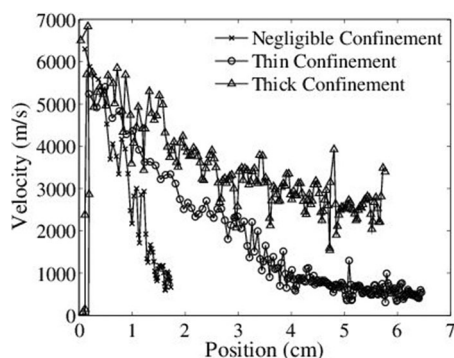


Figure 5. Results between negligible confinement, thick confinement, and thin wall confinement using AN/2 wt-% mineral oil showing the velocity as a function of position through the non-ideal explosive.

tions are changed. Figure 5 shows the reactive front velocity as it travels through AN/2 wt-% mineral oil for various confinement conditions. The condition emulating no confinement (thin plastic tube) showed deceleration of the overdriven reactive front much more rapidly when compared to the other confinement conditions. The radial loss of energy is greatest with conditions of little confinement and the failing reactive wave does not continue beyond 2 cm of the HME.

The difference in the failure dynamics for different confinement is due to energy loss from the reaction zone. In the thin wall confiners, there are more significant lateral losses due to plastic deformation and expansion. With sizing of the HME below the critical diameter, the energy loss due to plastic deformation of the confiner can surpass the amount of energy supplied to the leading shock by the reaction zone. The reactive front weakens until the reactive wave can no longer be sustained and the shock wave decouples from the reaction zone.

Unlike with thin wall confinement, the velocity of the thick wall confiner never dropped below 1000 m s⁻¹. The transition zone for a decoupled shock wave seen with the thin wall confiners was not evident with the thick wall confiners. This indicates that although the reactive wave is weakening, with a decreasing velocity, complete failure never occurs for thick walled confiners although the propagation speed is far from C-J, as might be expected. Tabulated values of the velocities for each case can be found in the Supporting Information (Table S2).

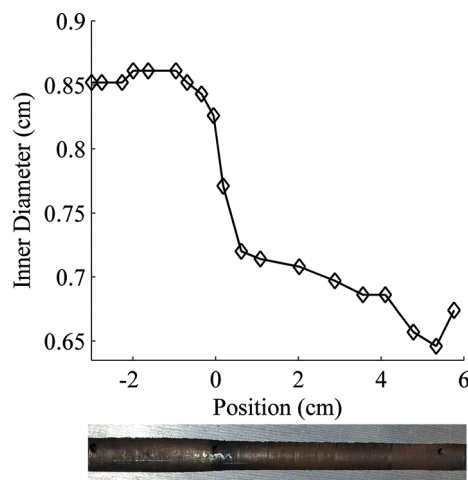


Figure 6. Measurement of the I.D. of the recovered thick wall confiner (top) where $x=0$ is the location that the detonation transfers to the non-ideal explosive along with the cross-section of the thick-wall confiner cut in half used to measure the inner diameter I.D. (bottom).

The amount of deformation that occurs within the thick wall confiner should depend on the amount of energy lost from the reaction zone. Energy is required to result in expansion of the confiner. Measuring the amount of deformation that occurred after the HME reactive front would verify whether or not a reactive front (approaching a steady detonation) occurred through the entire length of the confiner.

The thick-wall confiners were cut in half to produce one side that would allow for the measurement of the inner diameter, as seen in the bottom of Figure 6, to determine the expansion from the original diameter of 6.35 mm. Inner diameter measurements (top of Figure 6) showed that a coupled reactive wave occurred through the entire length of AN/2 wt-% mineral oil, as the measured I.D. never dropped below 6.46 mm. The fiber optic cable placed at the end of the HME in the thick wall confiner was also triggered indicating that a luminous reaction occurred through the entirety of the sample.

Previous work has shown that energy lost, due to expansion of the confiners, is distributed in front of the detonation by pressure waves when the sound speed of the confiner is larger than the velocity of the explosive [20]. The speed of sound for steel is 5790 m s⁻¹ [21]. The reactive wave front velocities measured in this work propagated at values below the sound speed of the steel confiners, allowing for the energy lost due to deformation of the confiners to be distributed in front of the detonation front. The transported energy into the walls could of course have an effect on the reactive wave velocity. It was also shown by Jackson et al. [20] that when energy transport within the confiner occurs, increasing the confiner thickness increases the detonation velocity of ammonium nitrate/fuel oil. In this work, increasing confinement thickness showed a similar trend as the sustainment of the reactive wave was shown to in-

crease. Consequently, simulations of these data should certainly account for confiner wall thickness and wall material properties.

3.4 Effect of Attenuator Thickness with AN/2 wt-% Diesel Fuel

Experiments were also performed using PMMA (density of 1.18 g cm^{-3}) attenuators in thin and thick wall confiners with various attenuator thicknesses. These experiments allow for examination of the transient dynamics as applied shock strength is varied. The strength of the shock wave transmitted to the HME (AN/2 wt-% diesel fuel) is dependent on the thickness of the attenuator. Thicker attenuators result in weaker applied shock waves. The weaker shock waves should lower initial reactive wave velocities in the HMEs. Associated with the weaker shock waves across the attenuator is an increase in curvature to the reaction front that leads to a two-dimensional shock initiation. However, this complexity is still acceptable for the purpose of these experiments due to the ability of simulations to replicate two-dimensional reaction zone curvature for rate law calibration. The use of an attenuator can also allow for the run-to-failure distance to be obtained as a function of attenuation when thin wall confiners are used, similar to "Pop-plots" for shock initiation.

3.4.1 Thick Wall Confinement

Using thick wall confinement with AN/2 wt-% diesel fuel, attenuators 2, 4, and 8 mm thick were tested along with a base case without attenuation. As shown in Figure 7, the velocity without an attenuator produced a higher initial wave velocity. Using the 2 mm thick attenuator reduced the initial reactive wave velocity, but the deceleration is seen to be similar to the deceleration without an attenuator. Increasing the attenuator thickness to 4 mm showed very little difference compared to the 2 mm case (not shown). It could be expected that a lower initiating reactive wave velocity would be observed with a slightly thicker attenuator. However, the additional 2 mm thickness of the attenuator may not have as large of an effect on the leading shock strength compared to just the effect of having the presence of the attenuator of any thickness due to impedance mismatching effects. With a doubling of the attenuator thickness to 8 mm from 4 mm, the largest decrease in initiating reactive wave velocity is seen. However, the deceleration of the reactive wave in all three cases has a common slope indicating that the dynamics occurring (specifically the losses in energy to deformation of the confiner walls) are similar. The key difference is that the initial reactive wave velocity is dependent on the incoming shock wave strength (attenuator thickness), which was expected.

Results for all cases show a nearly steady wave velocity near 2000 m s^{-1} . The steady detonation velocity was calculated using CHEETAH to be 1865 m s^{-1} for AN/2 wt-%

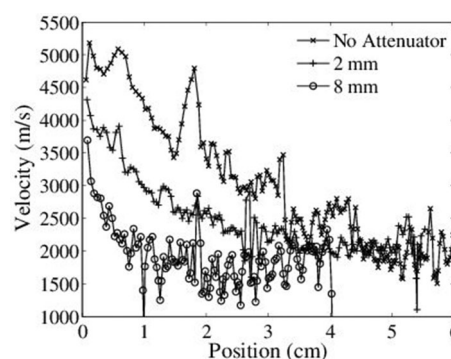


Figure 7. Results showing velocity of a detonation front through AN/2 wt-% diesel fuel with various attenuator thicknesses to alter the overdriven shock strength in thick-wall confiners.

diesel. With the thick wall confinement, a steady wave may therefore be sustainable. The fiber optic cables placed at the end of the confiners indicated that a reactive wave propagated through the entire HME sample. Consequently, there was no recovery of unreacted HME for any of the thick wall confinement experiments. Failure position and average velocities at those positions can be found in the Supporting Information (Table S2).

3.4.2 Thin Wall Confinement

Experiments were also conducted in thin wall confiners. Attenuators of different thicknesses (0, 1, 4, and 8 mm) were used with a HME composition of AN/2 wt-% diesel fuel. Decreased leading reactive wave velocities were observed with thicker attenuators similar to thick wall confinement experiments. The deceleration of the reaction front was similar between each case, with the difference in leading velocity proportional to the transmitted shock strength. As observed in previous results with thin wall confinement, complete failure of the reactive wave occurred along with the decoupling of a shock wave. A run-to-failure (RTF) distance is observed to depend on the attenuator thickness (leading shock strength), as shown in Figure 8. The case

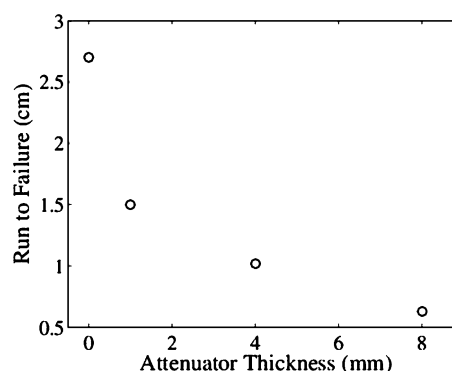


Figure 8. Run to failure as a function of attenuator thickness in a thin steel wall confiner for AN/2 wt-% diesel fuel.

without an attenuator was able to sustain the reaction the furthest through the HME, whereas the cases with attenuation showed a linear relationship between the RTF distance and the attenuator thickness. The RTF distance could be beneficial for calibrating a model of AN/2 wt-% diesel fuel in a thin wall confiner. Again, the large drop from no attenuator to a thin attenuator is attributed to impedance mismatch effects.

4 Conclusions

A unique method was developed to characterize the failure dynamics of HMEs with small sample sizes. The experimental work presented could be used for calibration of models using hydrocodes such as Sandia's CTH [22] or other shock physics code. The calibrated models could then be compared to large scale data for validation. If successful, it would show that this small scale experimental technique can be used for the characterization of HMEs and still be valid for large scale configurations. Regardless, this experiment is useful for improving the understanding of detonation failure in HMEs.

Experiments were performed using AN with diesel fuel and mineral oil. High resolution spatial measurements of the position and velocity were attained indicating factors such as chemical composition, confiner thickness, and initiating shock wave strength all affect the detonation failure dynamics. Thin wall experiments showed that stoichiometric compositions sustained a coupled reactive wave (approaching a steady detonation) further through the HMEs. Various confinement conditions used with AN/2 wt-% mineral oil showed how confinement had an effect on sustaining a coupled reactive wave (approaching a steady detonation) through a HME. Complete failure of the detonation was accompanied by a decoupling shock wave with thin wall confinement. It was shown that the thick wall confiner sustained the reactive wave through the entire length of HME by limiting the lateral loss of energy compared to the thin wall confinements and likely propagating energy ahead of the shock wave. Many other combinations of materials can now be quickly and conveniently considered.

The strength of the shock wave transmitted to the HME corresponded to the resulting initial reactive wave speed. In thin wall confinement, it was shown that the run-to-failure distance increased as the attenuator length decreased. Higher initiating shock strengths yielded additional energy for sustaining the reactive wave further into the HME. This experimental technique shows potential to reduce the time and cost required to dynamically characterize HMEs and rapidly characterize a variety of materials and confinement conditions over a broad parameter space. It is a useful tool for assessing the detonability of HMEs with only a few grams of material.

Acknowledgments

This project was funded by the Department of Homeland Security through the Center of Excellence for Explosive Detection, Mitigation, and Response under award number 080409/0002251. Discussions with Dr. Blaine Asay were also very useful.

References

- [1] W. M. Howard, L. E. Fried, P. C. Souers, Modeling of Non-Ideal Aluminized Explosives, *AIP Conference Proceedings*, 27 June – 2 July, **2000**, 505.1 p. 389.
- [2] A. Miyake, H. Echigoya, H. Kobayashi, T. Ogawa, K. Katoh, S. Kubota, Y. Wada, Non-Ideal Detonation Properties of Ammonium Nitrate and Activated Carbon Mixtures, *Int. J. Mod. Phys. B* **2008**, 22, 1319–1324.
- [3] S. I. Jackson, C. B. Kiyanda, M. Short, Experimental Observations of Detonation in Ammonium-nitrate-fuel-oil (ANFO) Surrounded by a High-speed, Shockless, Aluminum Confiner, *Proc. Combust. Inst.* **2011**, 33, 2219–2226.
- [4] A. Miyake, K. Takahara, T. Ogawa, Y. Ogata, Y. Wada, H. Arai, Influence of Physical Properties of Ammonium Nitrate on the Detonation Behavior of ANFO, *J. Loss Prevent. Process Indust.* **2001**, 14, 533–538.
- [5] F. W. Sandstrom, R. L. Abernathy, M. G. Leone, M. L. Banks, Diameter Effect and Detonation Front Curvature of Ideal and Non-ideal Explosives, *AIP Conference Proceedings*, 27 June–2 July, **2000**, 505 p. 825–828.
- [6] B. M. Dobratz, *LLNL Handbook of Explosives*, Report UCRL-52997, Lawrence Livermore National Laboratory, Livermore, CA, USA, **1981** (updated **1985**).
- [7] C. H. Johansson, P. A. Persson, in: *Detonics of High Explosives*, Academic Press, London, **1970**.
- [8] N. J. Burnside, S. F. Son, B. W. Asay, P. M. Dickson, Deflagration to Detonation Experiments in Granular HMX, *1997 Joint Army, Navy, NASA, Air Force (JANNAF) CS/Propulsion Systems Hazards Subcommittee Meeting*, West Palm Beach, FL, USA, 27–31 October, **1997**.
- [9] E. L. Lee, C. M. Tarver, Phenomenological Model of Shock Initiation in Heterogeneous Explosives, *Phys. Fluids* **1980**, 23, 2362–2372.
- [10] R. Menikoff, M. S. Shaw, Review of the Forest Fire Model for High Explosives, *Combust. Theory Model.* **2008**, 12, 569–604.
- [11] R. Menikoff, M. S. Shaw, Reactive Burn Models and Ignition & Growth Concept, *EPJ Web of Conferences*, **2010**, 10, p. 00003.
- [12] D. L. Robbins, S. A. Sheffield, D. M. Dattelbaum, N. Velisavljevic, D. B. Stahl, Equation of State of Ammonium Nitrate, *AIP Conference Proceedings*, 28 June–3 July, **2009**, 1195, p. 552–555.
- [13] E. J. Cart, R. H. Granholm, V. S. Joshi, H. W. Sandusky, R. J. Lee, Measurement of Ignition and Reaction Parameters in Non-Ideal Energetic Materials, *AIP Conference Proceedings*, 31 July–5 August, **2006**, 845 p. 1045–1048.
- [14] V. S. Bozic, D. D. Blagojevic, B. A. Anicin, Measurement System for Determining Solid Rocket Propellant Burning Rate using Reflection Microwave Interferometry, *J. Propul. Power* **1997**, 13, 457–462.
- [15] G. F. Cawsey, J. L. Farrands, S. Thomas, Observations of Detonation in Solid Explosives by Microwave Interferometry, *Proc. R. Soc. Lond.: Math. Phys. Eng. Sci.* **1958**, 248, 499–521.
- [16] M. A. Cook, R. L. Doran, G. J. Morris, Measurement of Detonation Velocity by Doppler Effect at 3-centimeter Wavelength, *J. Appl. Phys.* **1955**, 26, 426–428.

- [17] V. E. Zarko, D. V. Vdovin, V. V. Perov, Methodical Problems of Solid-Propellant Burning-rate Measurements Using Microwaves, *Combust. Explosion Shock Waves* **2000**, 36, 62–71.
- [18] B. A. Anicin, B. Jojic, D. Blagojcevic, M. Adzic, V. Milosavljevic, Flame Plasma and the Microwave Determination of Solid-Propellant Regression Rates, *Combust. Flame* **1986**, 64, 309–319.
- [19] L. E. Fried, W. M. Howard, P. C. Souers, *Cheetah 6.0 User's Manual*, Lawrence Livermore National Laboratory, Livermore, CA, USA, **2010**.
- [20] S. I. Jackson, C. B. Kiyanda, M. Short, Precursor Detonation Wave Development in ANFO Due to Aluminum Confinement, *14th International Detonation Symposium*, Coeur d'Alene, ID, USA, 11–16th July, **2010**.
- [21] *CRC Handbook of Chemistry and Physics*, 90edth edCRC Press, Boca Raton, FL, **2009**.
- [22] D. A. Crawford, A. L. Brundage, E. N. Harstad, E. S. Hertel Jr., R. G. Schmitt, S. C. Schumacher, J. S. Simmons, *CTH User's Manual and Input Instruction*, Sandia National Laboratories, Albuquerque, NM, USA, **2011**.

Received: April 11, 2013

Revised: May 14, 2014

Published online: July 30, 2014